molecules

MDPI

Review

Synthesis and Structural and Optical Behavior of Dehydrohelicene-Containing Polycyclic Compounds

Md. Imrul Khalid [1,2], Mohamed S. H. Salem [1,3] and Shinobu Takizawa [1,*]

[1] SANKEN, Osaka University, Mihogaoka, Ibaraki-shi 567-0047, Osaka, Japan; imrul43@sanken.osaka-u.ac.jp (M.I.K.); mohamedsalem43@sanken.osaka-u.ac.jp (M.S.H.S.)
[2] Organic and Carbon Nanomaterials Unit, Okinawa Institute of Science and Technology Graduate University, 1919-1 Tancha, Onna-son, Kunigami-gun, Okinawa 904-0495, Japan
[3] Pharmaceutical Organic Chemistry Department, Faculty of Pharmacy, Suez Canal University, Ismailia 41522, Egypt
* Correspondence: taki@sanken.osaka-u.ac.jp

Abstract: Dehydrohelicene-based molecules stand out as highly promising scaffolds and captivating chiroptical materials, characterized by their unique chirality. Their quasi-helical π-conjugated molecular architecture, featuring successively *ortho*-annulated aromatic rings, endows them with remarkable thermal stability and optical properties. Over the past decade, diverse approaches have emerged for synthesizing these scaffolds, reinvigorating this field, with anticipated increased attention in the coming years. This review provides a comprehensive overview of the historical evolution of dehydrohelicene chemistry since the pioneering work of Zander and Franke in 1969 and highlights recent advancements in the synthesis of various molecules incorporating dehydrohelicene motifs. We elucidate the intriguing structural features and optical merits of these molecules, occasionally drawing comparisons with their helicene or circulene analogs to underscore the significance of the bond between the helical termini.

Keywords: dehydrohelicene; quasicirculene; helicenes; circulenes; nanographene; material-based applications; Scholl reaction; photophysical; chiroptical; synthesis

check for updates

Citation: Khalid, M.I.; Salem, M.S.H.; Takizawa, S. Synthesis and Structural and Optical Behavior of Dehydrohelicene-Containing Polycyclic Compounds. *Molecules* **2024**, *29*, 296. https://doi.org/10.3390/molecules29020296

Academic Editor: Giorgio Bencivenni

Received: 30 November 2023
Revised: 28 December 2023
Accepted: 3 January 2024
Published: 5 January 2024

Copyright: © 2024 by the authors. Licensee MDPI, Basel, Switzerland. This article is an open access article distributed under the terms and conditions of the Creative Commons Attribution (CC BY) license (https://creativecommons.org/licenses/by/4.0/).

1. Introduction

The exploration of stereochemistry has been a subject of enduring interest within the chemical community since Pasteur's landmark discovery of molecular chirality in the 19th century [1], followed by van 't Hoff and Le Bel's influential introduction of tetrahedral carbon [2,3]. Within the realm of molecular chirality, various types can be distinguished, including the well-known central, axial, helical, and planar chirality [4]. Twisting some one-dimensional nanocarbons out of planarity affects their optical and electronic properties and also induces chirality as shown in helically locked tethered twistacenes (twisted acenes) [5–7]. Certain compounds pose a challenge when attempting to classify them as purely axial or helical, as they exhibit characteristics of both. These molecules possess a rotational axis that contributes to their chirality, while simultaneously displaying a helical or spiral arrangement [8]. The most famous example of such scaffolds is the dehydrohelicenes, also described as quasicirculenes, which are *ortho*-fused polycyclic aromatic compounds in which the two helical termini are connected by a sigma bond [9–11]. They are derived from helicenes, which are compounds with a series of fused benzene or heterocyclic rings arranged in a helical or screw-like structure [12–16]. Dehydrohelicenes specifically contain double bonds in their helical structure, which introduces additional conjugation and alters their electronic properties compared to their fully saturated counterparts. Their unique scaffolds and chirality endowed them with various desirable photophysical, chiroptical, and electronic features that can be implemented in different material-based applications [17,18]. Although the first example of dehydrohelicenes was reported 50 years ago by Zander

and Franke, attention to their impact was not grabbed until recently [19]. This may be attributed to the fact that most dehydrohelicenes have been considered for a long time as side products in our quest for circulenes [20]. With the recent remarkable developments in the fields of renewable energy and materials applications of small organic molecules (SOMs) during the last two decades [21–24], dehydrohelicenes' characteristics were revisited, and their potential was re-evaluated for further innovative applications. Additionally, the advancements in measuring tools and chiroptical methods, such as Raman optical activity (ROA) [25], vibrational circular dichroism (VCD) [26–28], and circularly polarized luminescence (CPL) facilitated extensive investigations of the electronic and geometric merits of dehydrohelicenes, enabling a deeper understanding of their value [22,23,29–31]. Given their higher chiroptical responses and chiral stabilities, in many reported examples, compared to their helicene analogs, dehydrohelicenes received great attention in the last decade and various synthetic approaches were developed to access these scaffolds [10]. Dehydrohelicenes can be classified based on the incorporation of heteroatoms in their main skeleton into carbo-dehydrohelicenes and hetero-dehydrohelicenes (Figure 1). The first has a purely carbon-based ring structure, while the latter have heteroatoms incorporated into their ring, adding an extra layer of complexity and functionality [32–34].

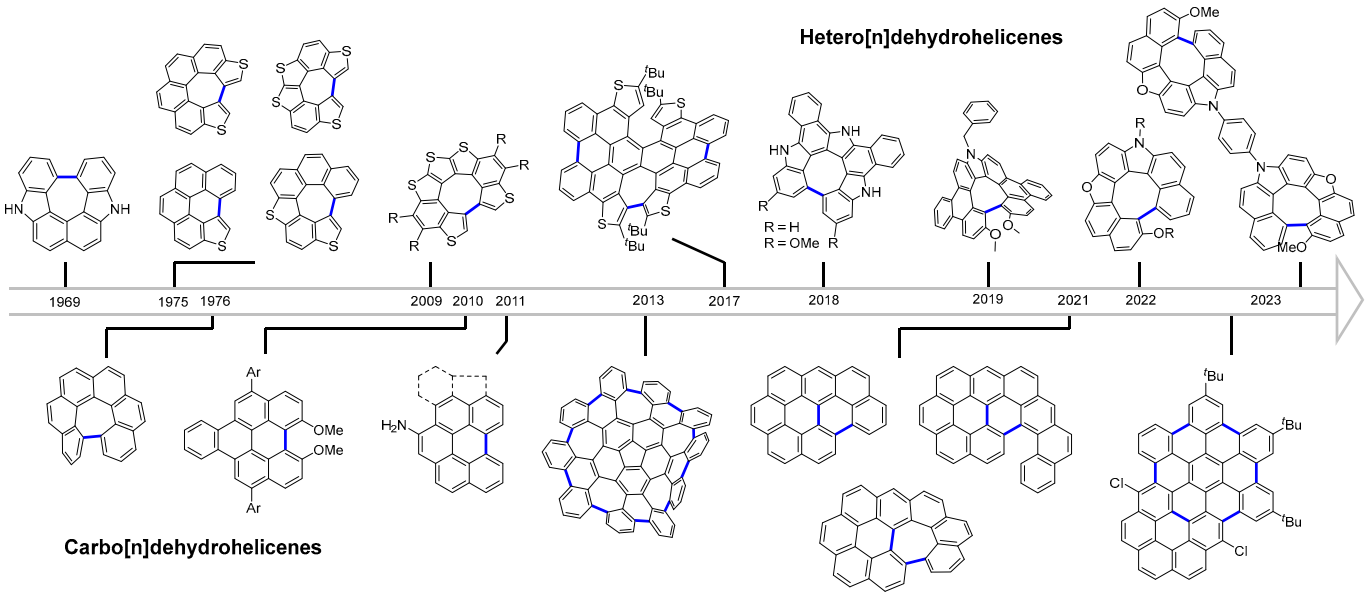


Figure 1. Comprehensive overview of the pivotal accomplishments in the chemistry of carbo[*n*]dehydrohelicenes and hetero[*n*]dehydrohelicenes over last 50 years: (**upper portion**) hetero[*n*]helicenes, distinguished by their incorporation of sulfur, nitrogen, or oxygen atoms into the helical framework, adding an extra layer of complexity and functionality; (**lower portion**) carbo[*n*]dehydrohelicenes, characterized by a dehydrohelicene scaffold composed solely of carbon and hydrogen atoms. Blue color indicates the sigma bonds connecting the two helical termini of dehydrohelicenes.

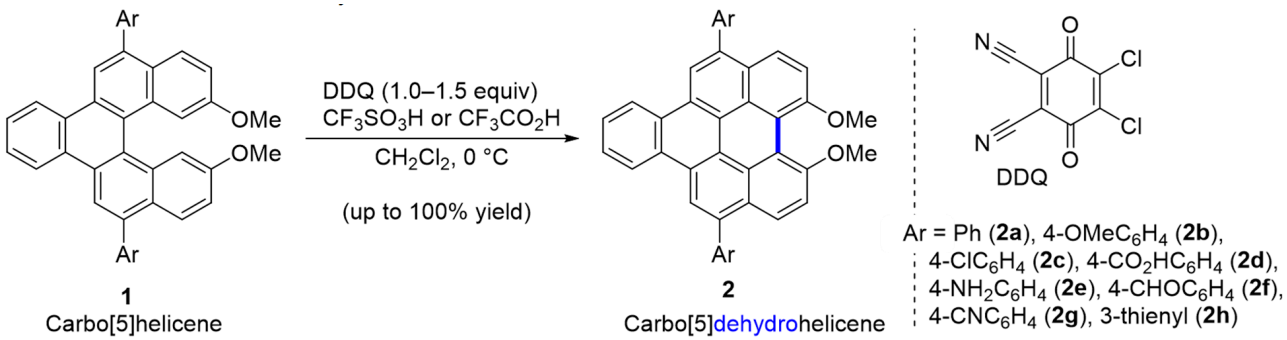
2. Carbo[*n*]dehydrohelicenes

Carbo[*n*]dehydrohelicenes represent a distinctive class of polycyclic aromatic hydrocarbons (PAHs) characterized by a cyclic scaffold featuring one or more double bonds arranged in a strained configuration. Notably, the structural composition of carbo[*n*]dehydrohelicenes is entirely carbon-based, devoid of any heteroatoms, wherein the constituent atoms are exclusively carbon [20]. This particular subset of dehydrohelicenes has saved considerable interest within the realm of organic chemistry, primarily owing to its exceptional molecular architecture [35]. In the burgeoning realm of nanographenes, their potential applications across diverse fields such as electronics, optoelectronics, and materials science have sparked a transformative revolution [36,37]. The controlled synthesis of nanographenes presents a

dual challenge and opportunity, allowing precise adjustment of properties based on size, shape, and functionalization [38–41]. Noteworthy, attention has recently been redirected to carbo[*n*]dehydrohelicenes, recognized as promising candidates due to their twisted structures, extensive conjugation, and inherent chirality in some cases [35,42]. The helical arrangement of dehydrohelicenes, driven by steric constraints and enhanced by optical activity, offers unique possibilities in asymmetric synthesis and as components for chiral sensors. Additionally, the absence of heteroatoms in their scaffold imparts unique chemical and physical properties, rendering this class of compounds particularly intriguing for exploration in the domains of materials science and bottom-up synthetic chemistry [43–45]. In the following sections, we will elucidate the seminal progressions in the synthesis and applications of carbo dehydrohelicenes, stratified according to the number of constituent rings within each dehydrohelicene scaffold.

2.1. Carbo[5]dehydrohelicenes

In a significant scientific investigation conducted by Chen and colleagues in 2010, the synthesis of carbo[5]dehydrohelicene **2** from the corresponding carbo[5]helicene derivatives **1** was reported [46]. The authors determined that the oxidative cyclodehydrogenation reactions of the helicenes **1** could be effectively achieved by employing the conditions established for Scholl reactions [47]. By utilizing either trifluoroacetic acid or trifluoromethanesulfonic acid with 2,3-dichloro-5,6-dicyano-1,4-benzoquinone (DDQ), carbo[5]helicene derivatives **1** was oxidized to form carbo[5]dehydrohelicenes **2** in excellent yields (Scheme 1).

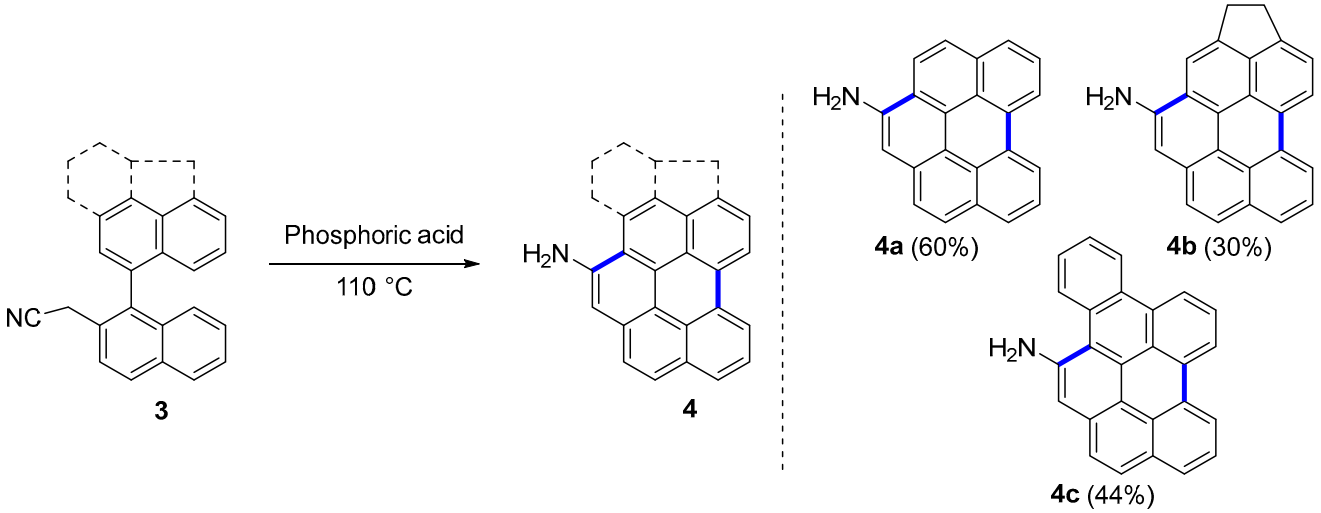


Scheme 1. Synthesis of carbo[5]dehydrohelicene derivatives via Scholl reaction.

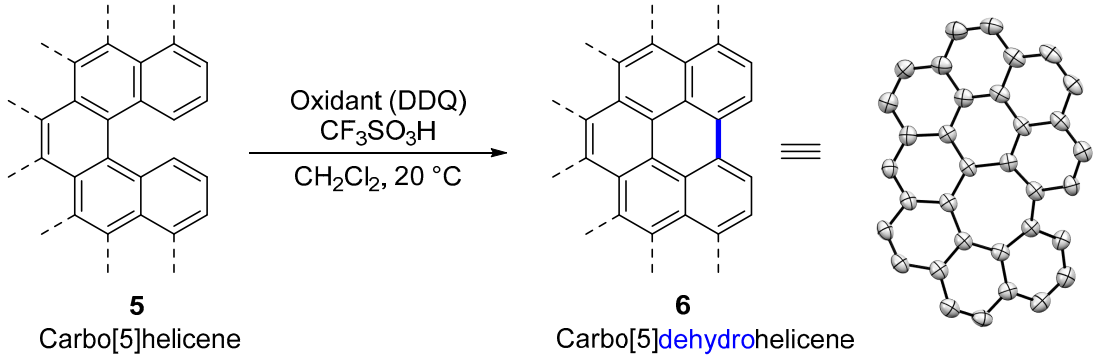
In 2011, Gaucher, Giner Planas, and coworkers reported novel molecular scaffolds of benzo[*ghi*]perylene derivatives **4** via a one-pot electrophilic aromatic substitution—Scholl reaction sequence. Under acidic conditions, the cyanomethylene pendant arm was installed on the binaphthyl moiety of **3** to promote the generation of the corresponding electrophile and ultimately give planar amino benzo[*ghi*]perylene units classified as carbo[5]dehydrohelicenes **4** in moderate to good yields (Scheme 2). Unlike their expectations, the polyphosphoric acid (PPA) was not able to afford the corresponding carbo[5]dehydrohelicenes **4** even at elevated temperatures 110 °C. The synergy of carborane and amino benzo[*ghi*]perylene moieties yielded distinctive 3D-planar molecular architectures. Photophysical analysis showcased that, while the absorption profile was primarily governed by the perylene-rigid fragment, both the carborane and organic subunits intricately influenced the emission characteristics of these novel structures [48].

More than 10 years later, Qiu et al. in 2021 developed a fascinating strategy to broaden the diversity of many carbo[*n*]helicenes **5** and give direct access to their corresponding carbo[*n*]dehydrohelicenes **6** through a unique oxidative cyclo-rearrangement reaction (Scheme 3). This Scholl cyclization process leads to the fabrication of a series of carbo[5]dehydrohelicene **6** driven by the gradual release of the strain of the highly distorted helicene skeletons. The authors employed a wide variety of acids, includ-

ing CF_3CO_2H, CH_3SO_3H, and CF_3SO_3H, along with DDQ as a crucial component to promote carbo[*n*]helicenes with (*n* = 7–9) to be firstly oxidized, cyclized, and subsequently rearranged into nanographenes with an unsymmetrical helicoid shape through sequential 1,2-migrations [49].



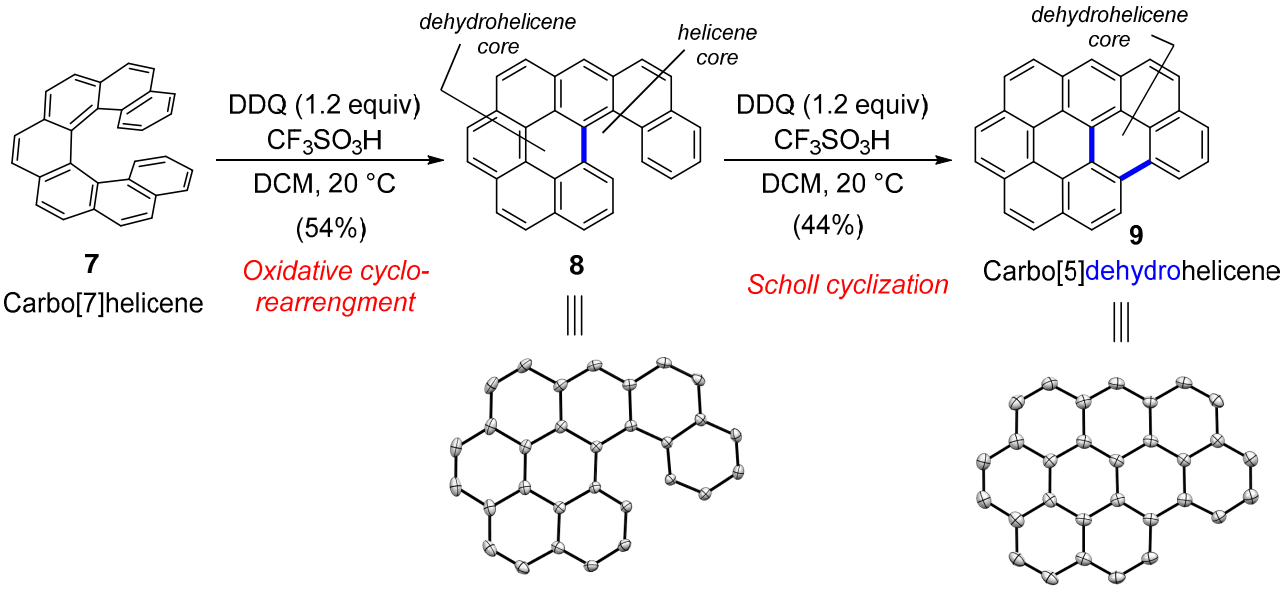
Scheme 2. Direct access to the unique architectures of amino benzo[*ghi*]perylene.



Scheme 3. Oxidative cyclo-rearrangement of carbo[*n*]helicenes into their corresponding carbo[5]dehydrohelicenes.

Upon oxidation by DDQ in the presence of CF_3SO_3H acidic additives, carbo[7]helicene **7** undergoes a cascade of oxidative cyclo-rearrangement followed by a Scholl cyclization reaction to afford the planar analogs of carbo[5]dehydrohelicenes **8** and **9** (Scheme 4) [49].

Most carbo[5]dehydrohelicene derivatives demonstrated commendable solubility in commonly used organic solvents. Compound **2a** exhibited a significant absorption band peaking at 436 nm in cyclohexane, demonstrating a pronounced bathochromic shift of 51 nm compared to benzo[*ghi*]perylene. This shift can be attributed to the extensively conjugated system of **2a** and, in some cases, the electron-donating effect of the methoxy groups in **2b** for example. Moreover, the maximum emission wavelength of **2a** was determined to be 478 nm, aligning with a distinct cyan fluorescence in the fluorescent spectrum [46]. To comprehensively investigate the photophysical properties of the other carbo[5]dehydrohelicene **2b**–**2h**, their UV–VIS absorbance, and photoluminescence (PL) patterns were studied in cyclohexane and exhibited comparable results to those of **2a** (Table 1). Importantly, the non-planarity of some substituted aromatic rings of the carbo[5]dehydrohelicene derivatives **2b** and **2f** resulted in minimal shifts in the emission wavelength. The quantum yields of the carbo[5]dehydrohelicenes varied considerably (Table 1), with electron-withdrawing groups generally yielding lower values, while electron-donating groups yielded higher values.



Scheme 4. Skeletal reconstruction of carbo[7]helicenes via a two-step oxidation protocol.

Table 1. The photophysical properties of carbo[5]dehydrohelicene **2** in cyclohexane.

Compound	Ar	Abs (nm)	Em (nm)	Quantum Yield ϕ
2a	phenyl	436	478	0.51
2b	4-$MeOC_6H_4$	436	489	0.78
2c	4-ClC_6H_4	435	480	0.45
2d	4-$CO_2HC_6H_4$	432	480	0.33
2e	4-$NH_2C_6H_4$	436	478	0.58
2f	4-$CHOC_6H_4$	433	489	0.40
2g	4-CNC_6H_4	433	480	0.47
2h	3-thienyl	438	481	0.75

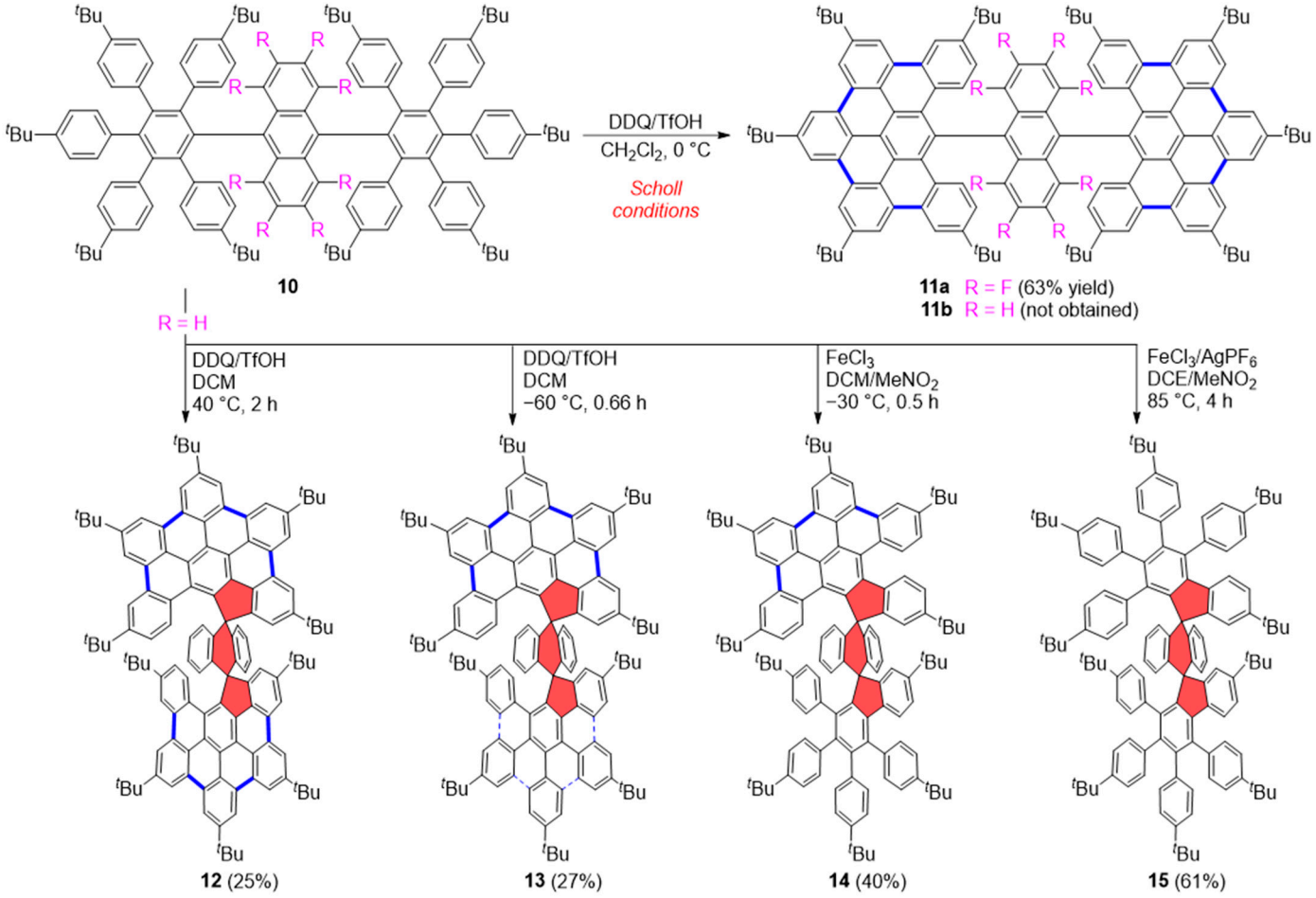
On the other hand, benzo[*ghi*]perylene derivatives **4** exhibited commendable photophysical properties, as outlined in Table 2, detailing the UV–VIS absorption and emission maxima for compounds **4a**–**4c** in THF. Notably, the incorporation of an electron-donating group, exemplified by $–NH_2$ in the structure of benzo[*ghi*]perylene, resulted in a discernible shift and broadening of both absorption and fluorescence spectra relative to pristine benzo[*ghi*]perylene. This observation aligns with the anticipated trends associated with the introduction of such functional groups into the benzo[*ghi*]perylene frameworks [50].

Table 2. The photophysical properties of carbo[5]dehydrohelicene **4** in THF.

Compound	Abs (nm)	Em (nm)	ε/M^{-1} cm^{-1}	Stokes Shift
4a	311	481	48,300	170
4b	309	475	17,300	166
4c	308	474	43,100	166

In 2023, Fernández and Martín demonstrated an innovative application of the Scholl reaction in the bottom-up synthesis of molecular nanographenes. Their investigation focused on the electronic effects of different starting substrates—specifically, anthracene versus octafluoroanthracene—and its control over the Scholl reaction. The study successfully yielded a series of spirocompounds (**12**–**15**) featuring a dehydrohelicene core with varying degrees of graphitization. The authors initially proposed the hypothetical synthesis of a helically arranged molecular nanographene **11b**, based on a 9,10-substituted anthracene with two dibenzo[fg,ij]phenanthro-[9,10,1,2,3-pqrst]pentaphene (DBPP) units **10b**. How-

ever, the optimized Scholl reaction conditions led to the isolation of partially graphitized intermediates (**13**–**15**) and the fully graphitized spironanographene **12** (Scheme 5) [51].

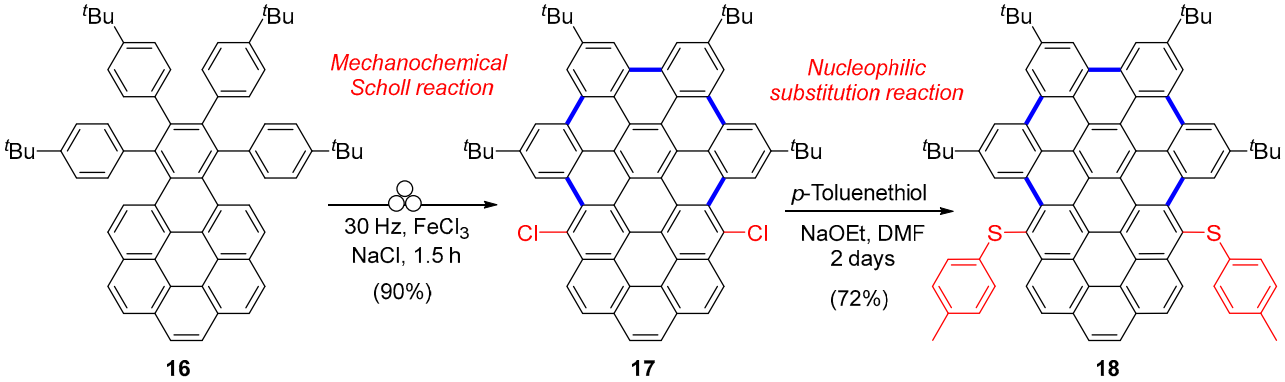


Scheme 5. Synthesis of various partially graphitized and fully graphitized spironanographene (dashed lines in compound **13** indicates that one of these bonds is not formed).

Electrochemical and photophysical investigations of *syn*-**12** unveiled disrupted electronic communication attributed to the emergence of two sp^3 spiranic carbons. The expanded band gap, in comparison with hexa-*peri*-hexabenzocoronene (HBC), manifested in distinctly separated reduction and oxidation potentials, accompanied by electronic bands experiencing a blue shift. Helically arranged nanographene **11a**, displaying acceptor characteristics, exhibited a comparatively lower first reduction potential in the CV, red-shifted bands in absorption and emission spectra, and a dual emission from the octafluoroanthracene fragment and the DBPP moieties [51].

In 2023, the Stuparu group reported a groundbreaking synthesis of precisely functionalizable curved nanographenes through graphitization-induced regioselective chlorination in a mechanochemical Scholl reaction [52]. Mechanochemistry, utilizing mechanical energy through grinding or milling, has recently emerged as a powerful synthetic tool, offering a sustainable approach to modifying chemical reactivity and product selectivity [53–59]. The mechanochemical Scholl reaction, facilitated by iron(III) chloride, demonstrated notable success [57,60–63], with precursor **16** undergoing regioselective chlorination to produce nanographene **17**. This solvent-free reaction employed a mixer mill with a ZrO_2 grinder jar and ZrO_2 balls, and sodium chloride as a milling auxiliary, with milling conducted for 1.5 h at a frequency of 30 Hz (Scheme 6). Characterization via MALDI-TOF mass spectrometry confirmed successful graphitization, revealing bis-chlorination during the process. Intriguingly, the graphitization step activated adjacent positions for chlorination,

resulting in chlorinated curved nanographenes. This regioselective chlorination presents an opportunity for atomically precise functionalization of the nanographene scaffold [52].

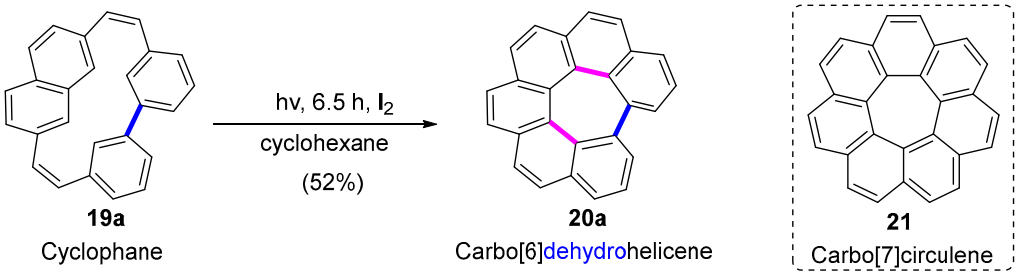


Scheme 6. Mechanochemical synthesis of functionalizable curved nanographenes.

UV–VIS spectroscopy of curved nanographenes **17** demonstrated moderate-intensity absorption bands at 400–550 nm with a significant 150 nm bathochromic shift compared to corannulene and coronene, indicating extended π-conjugation. The thioether-functionalized nanographene **18** exhibited the most red-shifted absorption band at 510 nm, attributed to the electron-donating nature of sulfur atoms. This observation suggests the potential for tuning the band-gap through post-synthesis functionalization. In fluorescence emission spectroscopy, the nanographenes displayed emissive properties in the blue-green region of the electromagnetic spectrum [52].

2.2. Carbo[6]dehydrohelicenes

Jessup and Reiss got the first carbo[6]dehydrohelicene **20** upon irradiating a solution of the cyclophane diene **19** in the presence of iodine as an oxidant (Scheme 7). It's noteworthy, their focus was primarily directed towards the synthesis of carbo[7]circulene **21**, and they did not explore the optical or electronic features of this intriguing carbo[6]dehydrohelicene scaffold **20** [20].

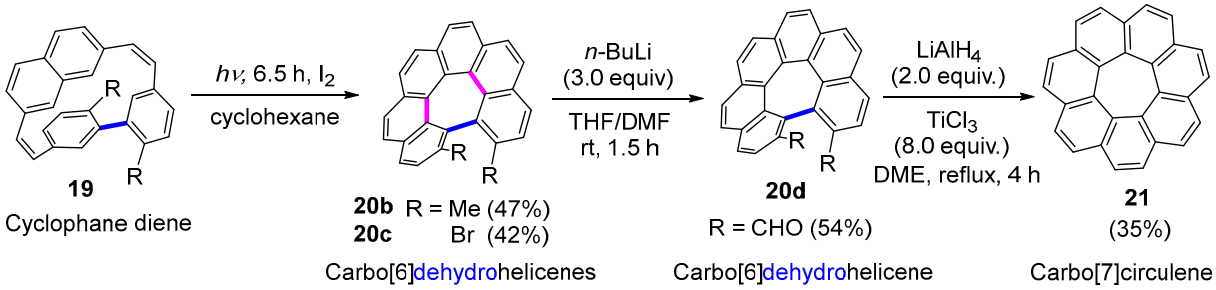


Scheme 7. Photochemical synthesis of carbo[6]dehydrohelicene.

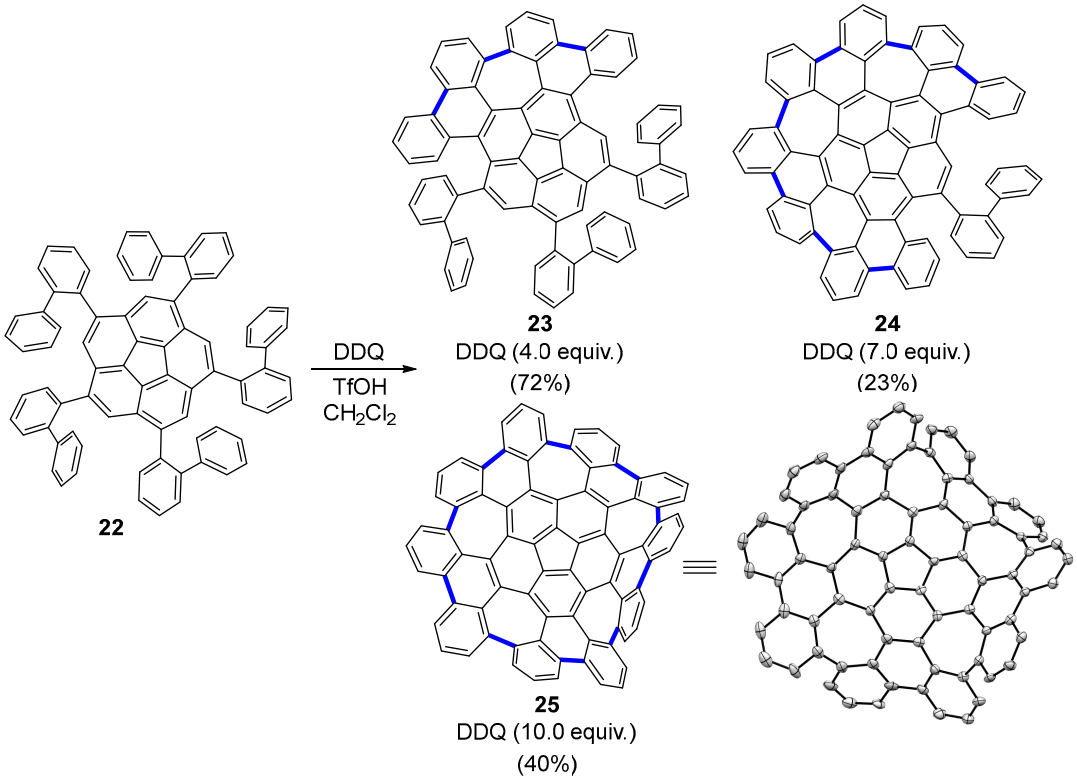
Later, Yamamoto and coworkers during their successful preparation of carbo[7]circulene **21**, confirmed the chiral nature of carbo[6]dehydrohelicenes **20**, and introduced another three derivatives of chiral carbo[6]dehydrohelicenes **20b**–**20d** upon irradiation of diene **19** (Scheme 8). However, the moderate racemization barriers of these carbo[6]dehydrohelicenes **20** (calculated barrier = 32.0 kcal mol^{-1}) hindered their further study and investigation [42].

In 2013, Itami and Scott reported an unconventional grossly warped nanographene with a dehydrohelicene core **25**, that showed superior behavior in terms of solubility, optical, and electronic features compared to other planar nanographene. The authors successfully synthesized this compound **25** from its precursor corannulene derivative **22** via Scholl reaction using 10 equivalents of DDQ (Scheme 9). The cyclization process affixes the five

polycyclic wing-like substituents to the hydrocarbon core then suture them together to generate ten new C–C bonds and five new seven-membered rings [35].



Scheme 8. Early synthesis of carbo[7]circulene and some carbo[6]dehydrohelicene derivatives.



Scheme 9. Preparation of a grossly warped nanographene with dehydrohelicene core.

The distinctive double-concave structure of compound **25** was explained by the dense accumulation of odd-membered-ring defects. The central corannulene moiety adopted a shallow bowl-shaped geometry with a depth of 0.37 Å. Notably, **25** exhibited chirality due to the presence of five helical moieties, each with either *M* or *P* chirality around the seven-membered ring, resulting in enantiomers with (*MPMPM*) and (*PMPMP*) configurations. While 25 exhibited minimal racemization barriers (calculated barrier of only 1.7 kcal mol^{-1}), limiting chiroptical investigations, the structural warping significantly enhanced the solubility and exerted prominent effects on both electronic and optical properties [35].

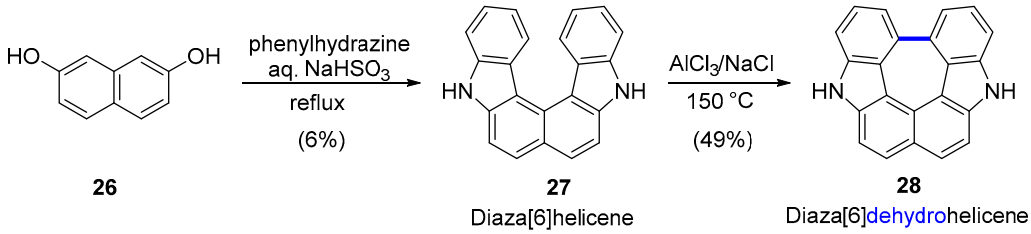
3. Hetero[*n*]dehydrohelicenes

Hetero[*n*]dehydrohelicenes, also referred to as quasi-heterocirculenes fall under the category of polycyclic heteroaromatics (PHAs) [17,18]. This distinct class of compounds features a sigma bond connecting the two helical termini of the corresponding hetero[*n*]helicene, resulting in exceptional photophysical, electronic, and chiroptical responses. Some hetero[*n*]dehydrohelicenes have reported a significant enhancement in chiral stability com-

pared to their hetero[*n*]helicene analogs, thereby amplifying their industrial value and broadening their range of applications [10]. These unique characteristics find applications in diverse material-based technologies, including organic light-emitting diodes (OLEDs) and field-effect transistors (FETs). The remarkable chiroptical properties of hetero[*n*]dehydrohelicenes, such as circular dichroism (CD) and circularly polarized luminescence (CPL), open avenues for applications in optical information storage and transfer [64]. The key distinction between hetero[*n*]dehydrohelicenes and their carbo- analogs lies in the incorporation of one or more heteroatoms into the dehydrohelicene scaffolds. This modification results in the modulation of their physical and optical characteristics, consequently altering electronic properties and expanding their utility [65–67]. Despite the promising potential in various applications, it is crucial to recognize that the realm of hetero[*n*]dehydrohelicene chemistry represents a relatively recent and burgeoning area of research. Realizing its full potential necessitates comprehensive investigations aimed at unraveling its intricate properties and delineating the scope of its applications across scientific and technological domains [68–70].

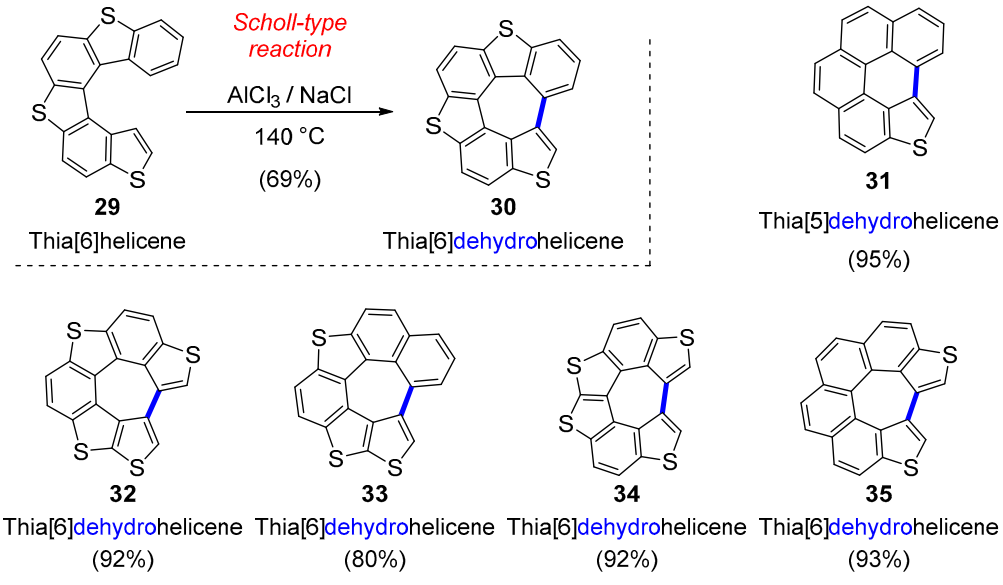
3.1. Hetero[5]dehydrohelicenes and Hetero[6]dehydrohelicenes

In 1969, Zander and Franke reported the first example of hetero[*n*]dehydrohelicene structures, representing the initial report among all dehydrohelicene core scaffolds. They employed a Scholl-type reaction to introduce diaza[6]dehydrohelicene **28**, synthesized from the precursor diaza[6]helicene **27** through $AlCl_3$-mediated terminal ring closure at 150 °C (Scheme 10) [19].



Scheme 10. First report of synthesizing dehydrohelicene scaffold using the chloraluminate method.

In 1975, Wynberg and co-workers used a similar Scholl-type approach to access various thiophene-based dehydro[5]helicenes **31** and dehydro[6]helicenes (**30**, **32**–**35**) in high yields (up to 95%) from the corresponding thia[*n*]helicenes **29** (Scheme 11) [9].

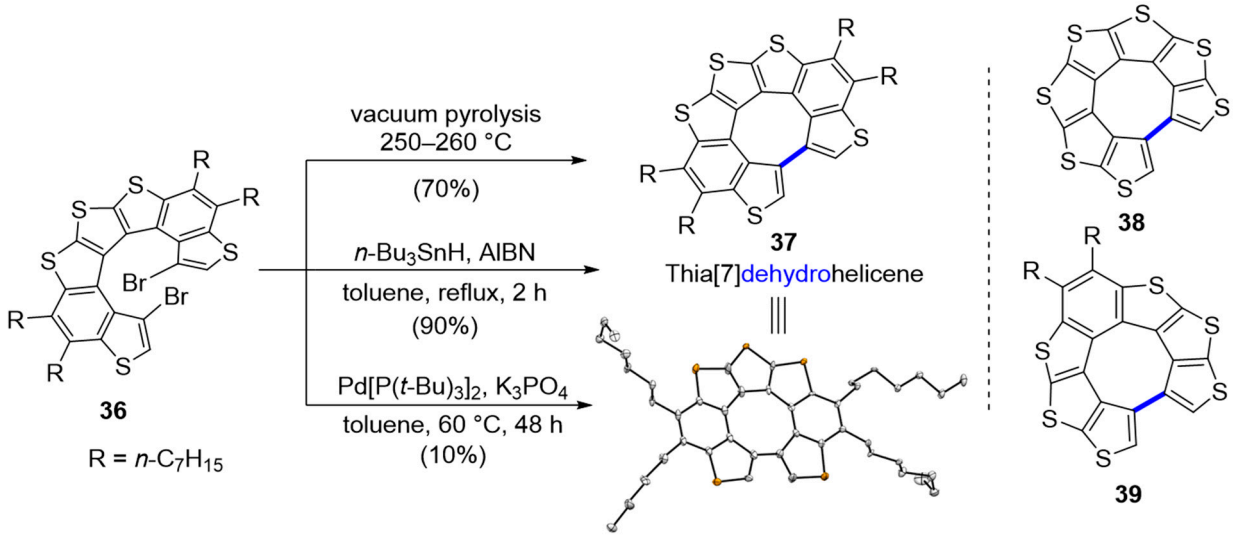


Scheme 11. Dehydrogenation of heterohelicenes by a Scholl-type reaction.

This study stood as one of the pioneering attempts to establish the sigma bond between the two helical termini of diverse hetero[*n*]helicenes, especially multi-thia[*n*]helicenes. Drawing insights from multiple trials and unsuccessful examples documented by the Wynberg group, it was evident that this intramolecular ring closure step was specifically confined to hetero[5]helicenes and hetero[6]helicenes [9,71].

3.2. Hetero[7]dehydrohelicenes

In 2009, Rajca described dehydrohelicene derivatives as quasi-circulenes for the first time, after getting three novel thiophene-based dehydro[7]helicene molecules **37**–**39** from their corresponding dibromo[7]helicenes **36** by three different methods; pyrolysis, tin-mediated, or palladium-mediated carbon-carbon bond forming reactions (Scheme 12) [11].



Scheme 12. Cyclization of thiophene-based [7]helicene at the two bromine-substituted termini.

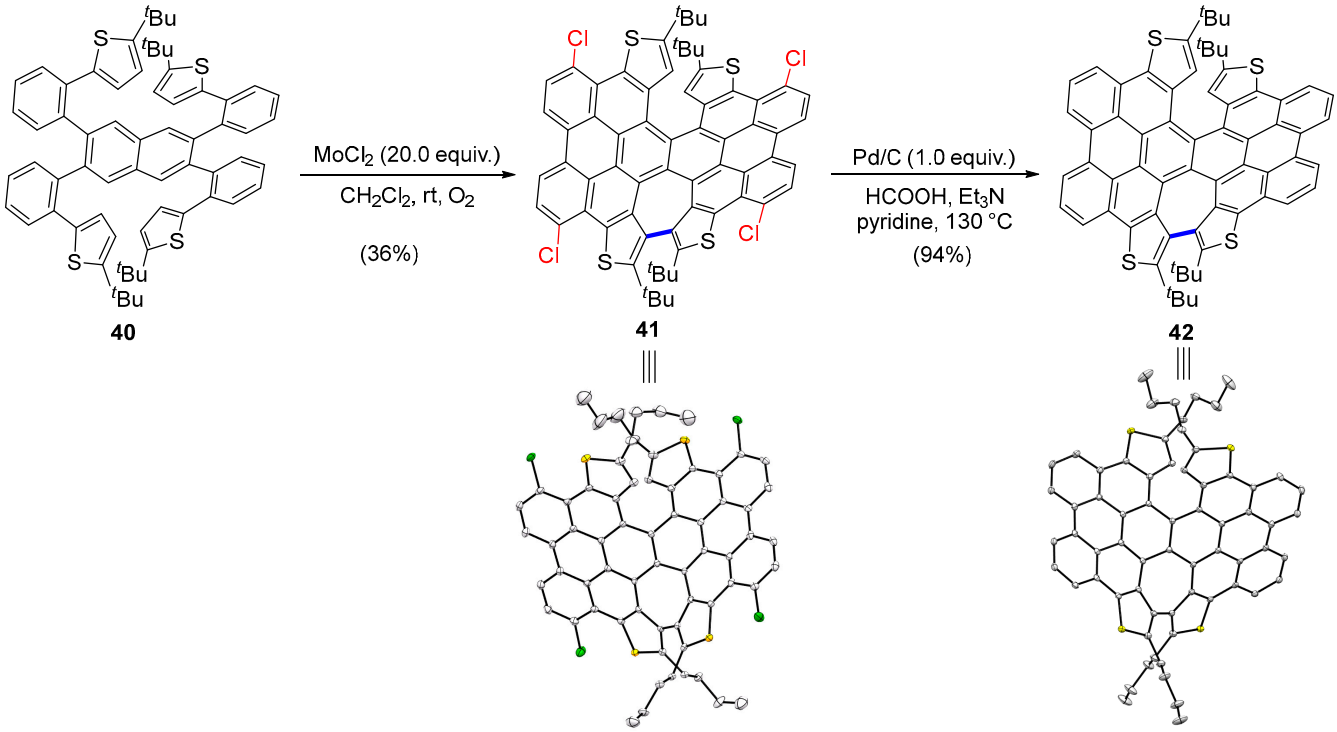
The interest in studying the photophysical properties of hetero[*n*]dehydrohelicenes dates back to 2009, when Rajca and coworkers studied the UV–VIS absorption of their three thiophene-based dehydro[7]helicene derivatives. The studied molecules **37**–**39** revealed good UV–VIS absorption properties characterized by a red-shifting with the increasing number of benzene rings and decreasing number of thiophene rings (Table 3) [11].

Table 3. The photophysical properties of various thia[7]dehydrohelicenes in cyclohexane.

Compound	λ_{max}/nm (ε/10^4 mol^{-1} dm^3 cm^{-1})			
37	244 (5.9)	326 (1.9)	338 (2.1)	348 (1.4)
38	265	-	-	-
39	256 (~3.3)	319 (~0.8)	333 (~0.8)	-

In 2017, Itami and Segawa reported the synthesis of a highly distorted saddle-helix molecule, **42**, with an exceptional racemization barrier (theoretically predicted to be 49.7 kcal·mol^{-1}). This represented a significant improvement compared to their previously reported grossly warped nanographene **25** (Scheme 9). The unique structure of **42** enabled the chiral HPLC resolution of both enantiomers for the first time, facilitating subsequent investigations into their chiroptical features. The synthesis involved a stepwise sequence, including a $MoCl_2$-mediated oxidative coupling of compound **40** with chlorination to cap reactive sites. Subsequent Pd-catalyzed dechlorination yielded compound **42** (Scheme 13). Electronic states of compounds **41** and **42** were studied using photophysical and electrochemical methods, revealing insights into the effects of chloride atom substitution and heptagonal ring formation [72].

The UV–VIS absorption spectra of **41** and **42** displayed two major absorption bands, with vibronic structures in longer-wavelength absorption and intense absorption around 400 nm. The absorption λ_{max} of **41** were observed at 518 nm, 486 nm, 455 nm, and 404 nm. In comparison, these λ_{max} were blue-shifted for **42**, appearing at 502 nm, 472 nm, 442 nm, and 394 nm. Fluorescence spectra exhibited a similar tendency with spectral shift compared to absorption pattern, with maxima at 530 and 566 nm for **41** (Φ_F = 0.37) and at 514 and 548 nm for **42** (Φ_F = 0.23). The circular dichroism (CD) spectrum displayed negative Cotton effects at 501 nm ($\Delta\varepsilon = -82\ M^{-1}\cdot cm^{-1}$) and 471 nm ($\Delta\varepsilon = -44\ M^{-1}\cdot cm^{-1}$) and positive Cotton effects at 421 nm ($\Delta\varepsilon = +111\ M^{-1}\cdot cm^{-1}$), 398 nm ($\Delta\varepsilon = +75\ M^{-1}\cdot cm^{-1}$), and 326 nm ($\Delta\varepsilon = +54\ M^{-1}\cdot cm^{-1}$) [72].



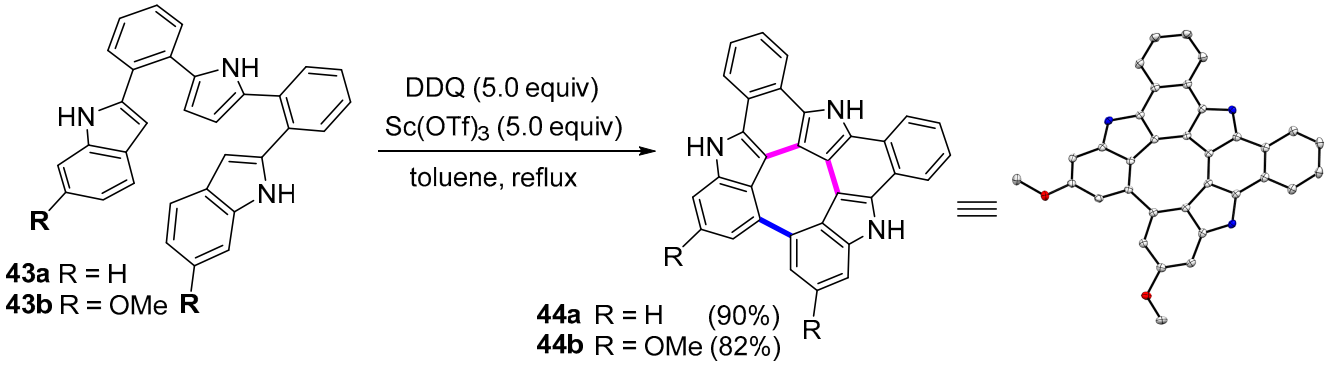
Scheme 13. Preparation of saddle-helix hybrid molecule with dehydrohelicene core moiety.

In 2018, Tanaka and Osuka introduced new triaza[7]dehydrohelicene molecules **44** that exhibit interesting photophysical properties. These scaffolds were synthesized in high yields via the oxidative fusion reaction of **43** using DDQ-Sc(OTf)$_3$ reagents in toluene under reflux conditions (Scheme 14). The UV–VIS absorption spectra of **44a** and **44b** exhibited a red-shifted absorption reaching up to λ_{max} = 470 nm. Additionally, their emission bands were shifted in a bathochromic way at 462 nm and 476 nm for compounds **44a** and **44b**, respectively, with a relatively large Stokes shift (1450 cm^{-1} in case of **44a**) probably due to their non-planar conformations. The very low racemization barriers of these structures (theoretically predicted to be ~5.2–6.0 $kcal\cdot mol^{-1}$) are an obstacle to the further investigation of their chiroptical merits [73].

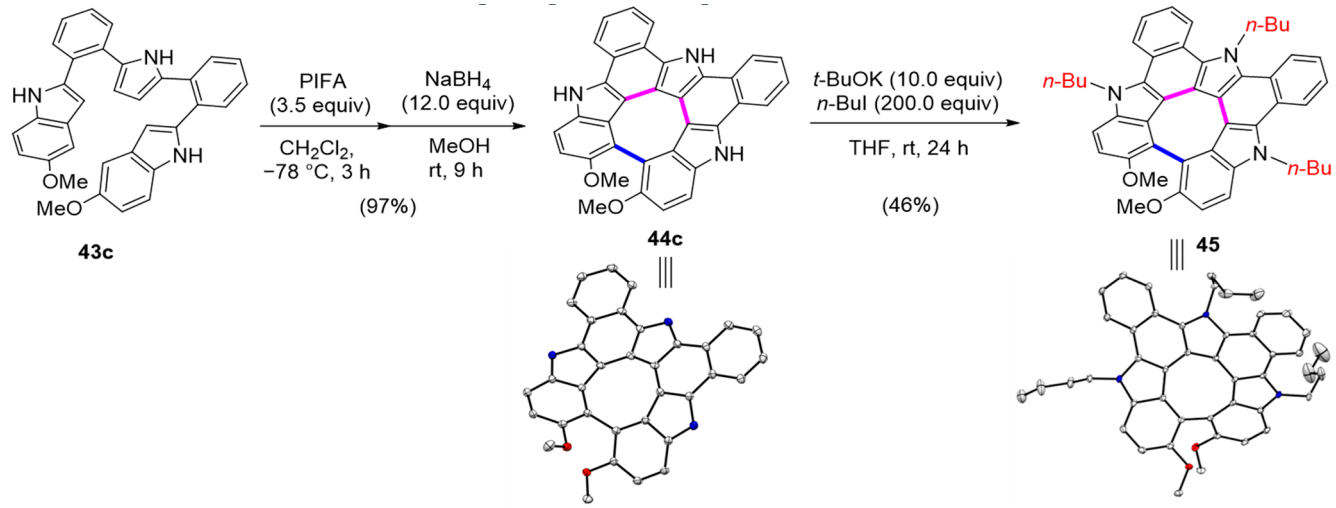
One year later, the same research group presented a modified iteration of their triaza[7]dehydrohelicene **45**, featuring a significantly high racemization barrier of approximately 40 $kcal\cdot mol^{-1}$. This advancement facilitated chiral resolution through HPLC and allowed an exploration of the compound's promising chiroptical features (Scheme 15). The CD spectra of **45** exhibited a mirror-image pattern, revealing a negative Cotton effect around 450 nm attributed to the (*M*) twisted form, as confirmed by comparison with the TD-DFT calculated CD spectrum. The UV–VIS absorption spectra of **45** demonstrated red-shifted absorption patterns compared to **44a** [74].

In 2020, Pittelkow and coworkers reported two interesting hetero[7]dehydrohelicenes **48a** and **48b** with three different heteroatoms (N, S, and O) incorporated into their scaffold

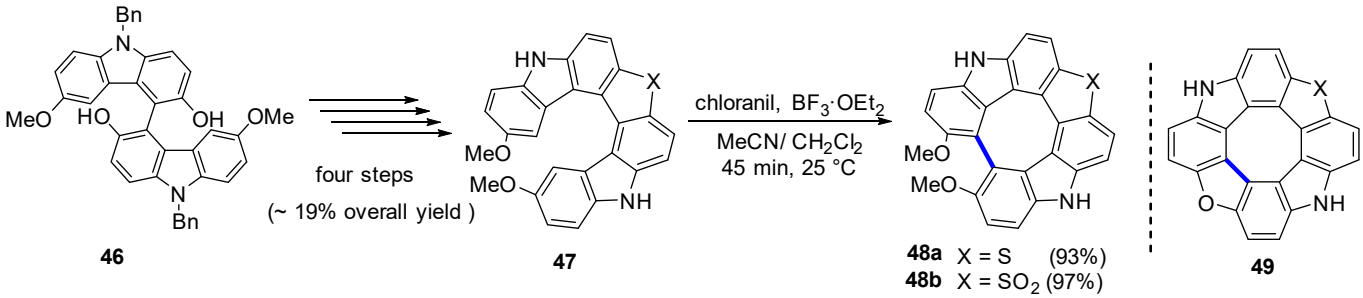
that showed improved optical and electrochemical features compared to the corresponding hetero[7]helicenes **47** and hetero[8]circulenes **49**. These two hetero[7]dehydrohelicenes **48a** and **48b** were synthesized in high yields via an intramolecular Scholl-type reaction upon treatment of the corresponding hetero[7]helicenes **47** with $BF_3{\cdot}OEt_2$ and chloranil. On the other hand, the helicene precursors **47** required a long synthetic protocol to be afforded from readily available substrates over four steps and affording 19% overall yield (Scheme 16). The photophysical properties, UV–VIS absorption and PL of these series were investigated in THF to reveal that the planarization of the scaffold showed a big impact on the photophysical properties. This was clearly indicated by the bathochromic shift in the onset of absorption shown in hetero[8]circulene **49** compared to hetero[7]dehydrohelicenes **48**. In spite of their estimated high chiral stability (~38.5 kcal·mol^{-1}), all attempts for their HPLC chiral resolution were unsuccessful preventing their further chiroptical study [75].



Scheme 14. Preparation of triaza[7]dehydrohelicene derivatives with low chiral stability.

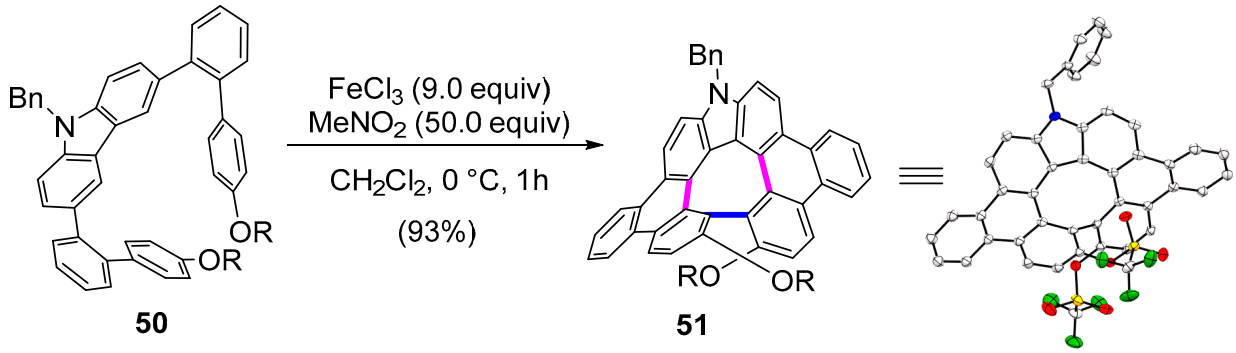


Scheme 15. Preparation of modified triaza[7]dehydrohelicene derivatives with high chiral stability.



Scheme 16. Preparation of unique dehydro[7]helicene derivatives with three different heteroatoms.

In 2021, Maeda and Ema reported another dehydro[7]helicene **51** that can be prepared via an intramolecular $FeCl_3$-mediated Scholl-type reaction from the precursor **50** (Scheme 17). The CPL of **51** was evaluated after HPLC chiral resolution, revealing $|g_{lum}|$ value of 2.5×10^{-4} at λ_{em} = 435 nm [76].



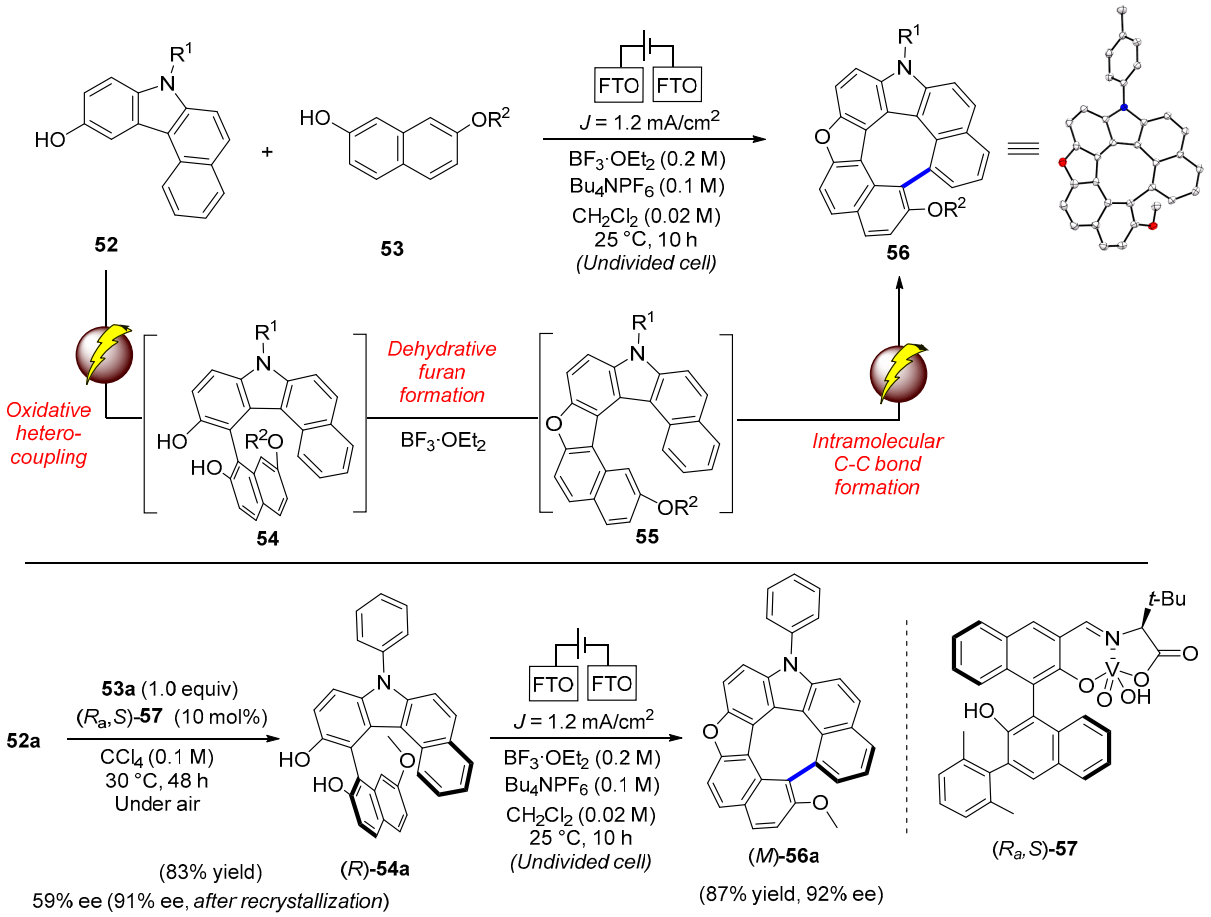
Scheme 17. Facile synthesis of aza[7]dehydrohelicene **51** via intramolecular Scholl-type reaction.

In 2022, Sasai and Takizawa introduced an efficient electrochemical sequential approach for the synthesis of diverse unsymmetrical oxaza[7]dehydrohelicenes **56**. Leveraging the readily available substrates: 3-hydroxy carbazoles **52** and 7-alkoxy-2-naphthol derivatives **53** as key coupling partners, their differential oxidation potentials (E_{ox} of **52** = +0.69 V, and E_{ox} of **53** = +1.32 V vs. Fc/Fc^+ in CH_2Cl_2) played a crucial role in orchestrating the chemoselectivity of the oxidative heterocoupling step, resulting in diol derivatives **54**. Subsequent dehydrative cyclization of these diols yielded oxaza[7]helicene derivatives **55**, followed by an intramolecular C-C bond formation between the helical termini, ultimately furnishing the corresponding oxaza[7]dehydrohelicene derivatives **56** (Scheme 18) [10].

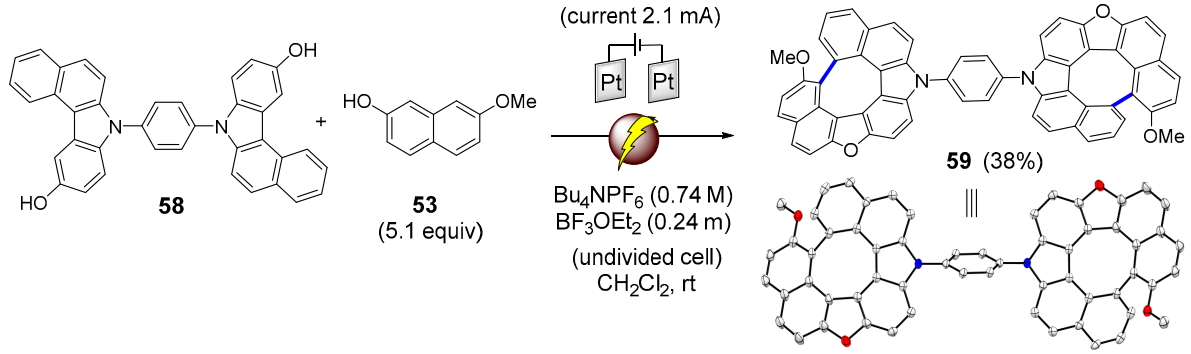
This protocol presents a highly efficient method for accessing diverse hetero[7]dehydrohelicenes **56** under mild conditions. The green electrochemical process sets itself apart by entirely eliminating metal waste, a notable departure from syntheses catalyzed by transitional metals [77–82]. The authors extended their approach to demonstrate the first enantioselective scalable synthesis of these dehydrohelicene molecules. This involves a stepwise hybrid chiral vanadium-catalyzed heterocoupling followed by electrochemical oxidative transformations (Scheme 18). To showcase the method's applicability for concise synthesis, a two-pot protocol was tested using commercially available substrates *p*-benzoquinone and *N*-phenyl-2-naphthylamine to afford oxaza[7]dehydrohelicene derivatives **56** with an overall yield of up to 55% [10]. Later, the same group updated these electrochemical conditions to overcome some limitations and improve the Faradic efficiency side by side with the sustainability of their method [83].

The synthesized oxaza[7]dehydrohelicenes **56** exhibited notable properties, including intense blue-colored circularly polarized luminescence ($|g_{lum}| \approx 2.5 \times 10^{-3}$ at 433 nm), the highest CPL observed for all dehydrohelicenes so far, and significant chiral stability. Racemization barrier studies indicated $\Delta G^{\ddagger} > 140$ kJ·mol^{-1} and $t_{1/2} >$ ca. 9.5×10^3 years at 25 °C, discernibly higher level of chiral stability when juxtaposed with its oxaza[7]helicene counterparts ($\Delta G^{\ddagger} > 110$ kJ·mol^{-1} and $t_{1/2} >$ ca. 5.7 days at 25 °C. The helical dyes within this study, demonstrated absorption within the wavelength range of 340–404 nm, coupled with fluorescence peaks at 420–450 nm [10].

In 2023, Salem and Takizawa employed this electrochemical approach to synthesize a novel heteronanographene with double chirality showcasing potential applications in various material-based technologies [84]. The study introduced an advanced Bayesian optimization (BO)-assisted screening of electrochemical conditions [85,86], efficiently identifying the optimum condition amidst the complexity of this sequential transformation with two functional sites and eight anodic events (Scheme 19). The unique architecture of this double oxaza[7]dehydrohelicene **59** exhibited high epimerization barriers (~34 kcal·mol^{-1}), addressing a significant challenge in many multiple heteronanographenes—the low chiral stability.



Scheme 18. Sequential electrochemical synthesis of oxaza[7]dehydrohelicene: (**upper**) electrochemical one-pot process; (**lower**) stepwise enantioselective synthesis via chiral vanadium-catalyzed hetero-coupling and electrochemical oxidative transformations.



Scheme 19. Data-driven electrochemical synthesis of double oxaza[7]dehydrohelicene.

The UV–VISs absorption of **59** was investigated using four solvents highlighting its excellent solubility in organic solvents, particularly advantageous for applications like solution-processed electronics [87,88]. The absorption patterns remained consistent across all solvents, with the highest absorbance at 323 nm and an optical bandgap (E_g) of 2.98 eV observed in chloroform. Emission spectra were recorded in pure chloroform to reveal bathochromic shifts with emission maxima at λ_{em} = 412 and 428 nm. The photoluminescence quantum yield (PLQY) of **59** measured at 30%, surpassing most reported chiral dehydrohelicenes. CD spectra indicate $|g_{abs}|$ values of 1.5×10^{-3}, 2.5×10^{-3}, and 2.1×10^{-3} at 398, 336, and 291 nm, respectively, for both enantiomers. Furthermore, $|g_{lum}|$

values for **59** measured as 1.5×10^{-3} at 430 nm, with (*P*,*P*)-**59** displaying a positive Cotton effect and (*M*,*M*)-**59** exhibiting a negative Cotton effect [84].

To this extent, it is evident that numerous synthetic approaches have been employed in the preparation of different dehydrohelicene-containing polycyclic compounds, as elucidated in Table 4. Most of these approaches relied on the Scholl reaction, either through utilizing an oxidizing agent such as (DDQ, chloranil, or $FeCl_3$) side by side with the acid to prepare different compounds at lower temperatures, or through a traditional Scholl reaction employing Lewis acids ($AlCl_3$) or protic acids (phosphoric acid) at elevated temperatures (>100 °C). Additionally, there was an example of employing the mechanochemical Scholl reaction for the production of compounds **17** and **18**. Some approaches relied on high temperatures (up to 290 °C), such as vacuum pyrolysis. Furthermore, metal-mediated oxidative coupling with metals such as tin, palladium, or molybdenum was introduced to furnish different compounds with dehydrohelicene core (**37**, **41**, and **42**). Other conditions for oxidative coupling using photochemical ring closure in the presence of iodine or hypervalent iodine (e.g., PIFA), have also been explored. Finally, a noteworthy example published by our groups employed electrochemical oxidation within a sequential framework to synthesize these compounds from readily available substrates.

Table 4. Several approaches and chiroptical properties (g_{abs}/g_{lum}) of dehydrohelicenes.

Synthetic Approaches	Conditions	Compounds	Chiroptical Features g_{abs}/g_{lum}
Scholl reaction	DDQ-mediated Scholl reaction	**2**, **6**, **11–14**, **23–25**	-
	Chloranil-mediated Scholl reaction	**48**	-
	$FeCl_3$-mediated Scholl reaction	**51**	$\lvert g_{lum} \rvert$ value of 2.5×10^{-4} at λ_{em} = 435 nm
	Phosphoric acid at 110 °C	**4**	-
	$AlCl_3$/NaCl at 140–150 °C	**28**, **30–35**	-
	Mechanochemical Scholl reaction	**17**, **18**	-
photochemical oxidative ring closure (*hv*, I_2)		**20**	-
Vacuum pyrolysis	180–290 °C under a vacuum $\leq$ 0.1 mTorr	**37**	-
Metal-mediated oxidative coupling	*n*-Bu_3SnH or $Pd[P(t\text{-}Bu)_3]_2$	**37**	-
	$MoCl_2$	**41**, **42**	Cotton effects at 501, 471, 421 nm
Oxidative fusion reaction	DDQ-$Sc(OTf)_3$	**44a**, **44b**	-
Hypervalent Iodine-induced Cyclization	PIFA/$NaBH_4$	**44c**	Cotton effects at 450, and 340 nm
Electrochemical oxidation		**56**, **59**	$\lvert g_{lum} \rvert$ of **56** = 2.5×10^{-3} $\lvert g_{lum} \rvert$ of **59** = 1.5×10^{-3}

Obviously, many of these dehydrohelicenes exhibited low racemization barriers, and in some cases (e.g., compounds **20** and **48**) researchers have faced challenges in achieving optical purity separation. This has hindered attempts to study their chiroptical properties. However, promising results have been demonstrated in studied examples such as compounds **51**, **56**, and **59** (Table 4).

4. Conclusions

This review encapsulates the synthesis and the photophysical and chiroptical characteristics of various molecules with dehydrohelicene cores. Initially considered as byproducts in the synthesis of circulenes half a century ago, dehydrohelicenes now exhibit significant potential in various material-based technologies. Many synthetic approaches to prepare dehydrohelicene-containing molecules have been discussed, yet many of them exhibit limitations such as low overall yields, harsh reaction conditions, or excessive use of oxidants. These challenges, coupled with difficulties in HPLC chiral resolution and low racemization barriers observed in certain instances, impede the progress of studies on the chiroptical behavior of these compounds. Despite recent advances introducing approaches that offer

the potential for enantioselective production of these scaffolds, there remains a substantial need to investigate additional methodologies and derivatives, aiming to diversify the landscape of this chemistry. This need is particularly pronounced given the distinctive value conferred by these scaffolds, characterized by quasi-helical π-conjugated systems, non-planarity, exceptional optical properties, and intrinsic chirality. Recent advancements in material chemistry and the renewed interest in CPL-responsive small organic molecules have prompted a decade of scholarly efforts focused on developing facile synthesis methods for dehydrohelicenes. These compounds have a huge promise in applications spanning liquid crystals, material dyes, asymmetric synthesis, molecular switches, polymers, photorefractive materials, self-assembly processes, photovoltaics, light-emitting devices.

Funding: This work was supported by JSPS KAKENHI Grant Numbers (21A204, 21H05217, and 22K06502), JST CREST (JPMJCR20R1), and Hoansha Foundation.

Data Availability Statement: Not applicable.

Acknowledgments: We acknowledge the past and current members of the Sasai and Takizawa groups for their efforts in developing new electrochemical approaches for synthesizing dehydrohelicene-containing molecules.

Conflicts of Interest: The authors declare no conflicts of interest.

References

1. Pasteur, L. Memoires sur la relation qui peut exister entre la forme crystalline et al. composition chimique, et sur la cause de la polarization rotatoire. *Compt. Rend.* **1848**, *26*, 535–538.
2. van't Hoff, J.H. A suggestion looking to the extension into space of the structural formulas at present used in chemistry, and a note upon the relation between the optical activity and the chemical constitution of organic compounds. *Arch. Neerl. Sci. Exactes Nat.* **1874**, *9*, 445–454.
3. Le Bel, J.A. Sur les relations qui existent entre les formules atomiques des corps organiques et le pouvoir rotatoire de leurs dissolutions. *Bull. Soc. Chim. Fr.* **1874**, *22*, 337–347.
4. Cahn, R.S.; Ingold, C.; Prelog, V. Specification of molecular chirality. *Angew. Chem. Int. Ed.* **1966**, *5*, 385–415. [CrossRef]
5. Bedi, A.; Gidron, O. The consequences of twisting nanocarbons: Lessons from tethered twisted acenes. *Acc. Chem. Res.* **2019**, *52*, 2482–2490. [CrossRef] [PubMed]
6. Bedi, A.; Shimon, L.J.W.; Gidron, O. Helically locked tethered twistacenes. *J. Am. Chem. Soc.* **2018**, *140*, 8086–8090. [CrossRef]
7. Bedi, A.; Gidron, O. Chiroptical properties of twisted acenes: Experimental and computational study. *Chem. Eur. J.* **2019**, *25*, 3279–3285. [CrossRef]
8. Rickhaus, M.; Mayor, M.; Juríček, M. Chirality in curved polyaromatic systems. *Chem. Soc. Rev.* **2017**, *46*, 1643–1660. [CrossRef]
9. Dopper, J.H.; Oudman, D.; Wynberg, H. Dehydrogenation of heterohelicenes by a Scholl type reaction. Dehydrohelicenes. *J. Org. Chem.* **1975**, *40*, 3398–3401. [CrossRef]
10. Khalid, M.I.; Salem, M.S.H.; Sako, M.; Kondo, M.; Sasai, H.; Takizawa, S. Electrochemical synthesis of heterodehydro[7]helicenes. *Commun. Chem.* **2022**, *5*, 166. [CrossRef]
11. Rajca, A.; Miyasaka, M.; Xiao, S.; Boratyński, P.J.; Pink, M.; Rajca, S. Intramolecular cyclization of thiophene-based [7]helicenes to quasi-[8]circulenes. *J. Org. Chem.* **2009**, *74*, 9105–9111. [CrossRef]
12. Gingras, M. One hundred years of helicene chemistry. Part 1: Non-stereoselective syntheses of carbohelicenes. *Chem. Soc. Rev.* **2013**, *42*, 968–1006. [CrossRef] [PubMed]
13. Gingras, M. One hundred years of helicene chemistry. Part 3: Applications and properties of carbohelicenes. *Chem. Soc. Rev.* **2013**, *42*, 1051–1095. [CrossRef] [PubMed]
14. Gingras, M.; Félix, G.; Peresutti, R. One hundred years of helicene chemistry. Part 2: Stereoselective syntheses and chiral separations of carbohelicenes. *Chem. Soc. Rev.* **2013**, *42*, 1007–1050. [CrossRef] [PubMed]
15. Shen, Y.; Chen, C.-F. Helicenes: Synthesis and applications. *Chem. Rev.* **2012**, *112*, 1463–1535. [CrossRef]
16. Salem, M.S.H.; Khalid, M.I.; Sasai, H.; Takizawa, S. Two-pot synthesis of unsymmetrical hetero[7]helicenes with intriguing optical properties. *Tetrahedron* **2023**, *133*, 133266. [CrossRef]
17. Borissov, A.; Maurya, Y.K.; Moshniaha, L.; Wong, W.-S.; Żyła-Karwowska, M.; Stępień, M. Recent advances in heterocyclic nanographenes and other polycyclic heteroaromatic compounds. *Chem. Rev.* **2021**, *122*, 565–788. [CrossRef]
18. Stępień, M.; Gońka, E.; Żyła, M.; Sprutta, N. Heterocyclic nanographenes and other polycyclic heteroaromatic compounds: Synthetic routes, properties, and applications. *Chem. Rev.* **2017**, *117*, 3479–3716. [CrossRef]
19. Zander, M.; Franke, W.H. Über Carbazolo-carbazole. *Chem. Berichte* **1969**, *102*, 2728–2738. [CrossRef]
20. Jessup, P.J.; Reiss, J.A.; Cyclophanes, V. Biphenylnaphthalenophanes and the synthesis of Hexa[7]circulene. *Aust. J. Chem.* **1976**, *29*, 173–178. [CrossRef]

21. Roncali, J.; Leriche, P.; Blanchard, P. Molecular materials for organic photovoltaics: Small is beautiful. *Adv. Mater.* **2014**, *26*, 3821–3838. [CrossRef] [PubMed]
22. Ma, J.-L.; Peng, Q.; Zhao, C.-H. Circularly polarized luminescence switching in small organic molecules. *Chem. Eur. J.* **2019**, *25*, 15441–15454. [CrossRef] [PubMed]
23. Mori, T. Frontiers of circularly polarized luminescence Chemistry of isolated small organic molecules. In *Circularly Polarized luminescence of Isolated Small Organic Molecules*; Springer: Singapore, 2020; pp. 1–10.
24. Wu, Z.-Y.; Xu, S.-L.; Yan, Q.-Q.; Chen, Z.-Q.; Ding, Y.-W.; Li, C.; Liang, H.-W.; Yu, S.-H. Transition metal–assisted carbonization of small organic molecules toward functional carbon materials. *Sci. Adv.* **2018**, *4*, eaat0788. [CrossRef] [PubMed]
25. Barron, L.D.; Hecht, L.; McColl, I.H.; Blanch, E.W. Raman optical activity comes of age. *Mol. Phys.* **2004**, *102*, 731–744. [CrossRef]
26. Stephens, P.J.; Devlin, F.J.; Pan, J.-J. The determination of the absolute configurations of chiral molecules using vibrational circular dichroism (VCD) spectroscopy. *Chirality* **2008**, *20*, 643–663. [CrossRef] [PubMed]
27. Kurouski, D. Advances of vibrational circular dichroism (VCD) in bioanalytical chemistry. A review. *Anal. Chim. Acta* **2017**, *990*, 54–66. [CrossRef] [PubMed]
28. Lakhani, A.; Malon, P.; Keiderling, T.A. Comparison of vibrational circular dichroism instruments: Development of a new dispersive VCD. *Appl. Spectrosc.* **2009**, *63*, 775–785. [CrossRef]
29. Sánchez-Carnerero, E.M.; Agarrabeitia, A.R.; Moreno, F.; Maroto, B.L.; Muller, G.; Ortiz, M.J.; de la Moya, S. Circularly polarized luminescence from simple organic molecules. *Chem. Eur. J.* **2015**, *21*, 13488–13500. [CrossRef]
30. Chen, N.; Yan, B. Recent theoretical and experimental progress in circularly polarized luminescence of small organic molecules. *Molecules* **2018**, *23*, 3376. [CrossRef]
31. Li, X.; Xie, Y.; Li, Z. The progress of circularly polarized luminescence in chiral purely organic materials. *Adv. Photonics Res.* **2021**, *2*, 2000136. [CrossRef]
32. Jakubec, M.; Storch, J. Recent advances in functionalizations of helicene backbone. *J. Org. Chem.* **2020**, *85*, 13415–13428. [CrossRef]
33. Liu, Z.; Fu, S.; Liu, X.; Narita, A.; Samorì, P.; Bonn, M.; Wang, H.I. Small Size, Big Impact: Recent Progress in Bottom-Up Synthesized Nanographenes for Optoelectronic and Energy Applications. *Adv. Sci.* **2022**, *9*, 2106055. [CrossRef]
34. Xu, X.; Müllen, K.; Narita, A. Syntheses and characterizations of functional polycyclic aromatic hydrocarbons and graphene nanoribbons. *Bull. Chem. Soc. Jpn.* **2020**, *93*, 490–506. [CrossRef]
35. Kawasumi, K.; Zhang, Q.; Segawa, Y.; Scott, L.T.; Itami, K. A grossly warped nanographene and the consequences of multiple odd-membered-ring defects. *Nat. Chem.* **2013**, *5*, 739–744. [CrossRef] [PubMed]
36. Hemminger, J.C.; Sarrao, J.; Crabtree, G.; Flemming, G.; Ratner, M. *Challenges at the Frontiers of Matter and Energy: Transformative Opportunities for Discovery Science*; USDOE Office of Science (SC): Germantown, MD, USA, 2015.
37. Gupta, A.; Sakthivel, T.; Seal, S. Recent development in 2D materials beyond graphene. *Prog. Mater. Sci.* **2015**, *73*, 44–126. [CrossRef]
38. Itami, K. Toward controlled synthesis of carbon nanotubes and graphenes. *Pure Appl. Chem.* **2012**, *84*, 907–916. [CrossRef]
39. Pozo, I.; Guitián, E.; Pérez, D.; Peña, D. Synthesis of nanographenes, starphenes, and sterically congested polyarenes by aryne cyclotrimerization. *Acc. Chem. Res.* **2019**, *52*, 2472–2481. [CrossRef]
40. Narita, A.; Wang, X.-Y.; Feng, X.; Müllen, K. New advances in nanographene chemistry. *Chem. Soc. Rev.* **2015**, *44*, 6616–6643. [CrossRef]
41. Jassas, R.S.; Mughal, E.U.; Sadiq, A.; Alsantali, R.I.; Al-Rooqi, M.M.; Naeem, N.; Moussa, Z.; Ahmed, S.A. Scholl reaction as a powerful tool for the synthesis of nanographenes: A systematic review. *RSC Adv.* **2021**, *11*, 32158–32202. [CrossRef]
42. Yamamoto, K.; Harada, T.; Okamoto, Y.; Chikamatsu, H.; Nakazaki, M.; Kai, Y.; Nakao, T.; Tanaka, M.; Harada, S.; Kasai, N. Synthesis and molecular structure of [7]circulene. *J. Am. Chem. Soc.* **1988**, *110*, 3578–3584. [CrossRef]
43. Toya, M.; Omine, T.; Ishiwari, F.; Saeki, A.; Ito, H.; Itami, K. Expanded [2, 1][n]Carbohelicenes with 15-and 17-Benzene Rings. *J. Am. Chem. Soc.* **2023**, *145*, 11553–11565. [CrossRef] [PubMed]
44. Chaolumen; Stepek, I.A.; Yamada, K.E.; Ito, H.; Itami, K. Construction of heptagon-containing molecular nanocarbons. *Angew. Chem. Int. Ed.* **2021**, *60*, 23508–23532. [CrossRef] [PubMed]
45. Miera, G.G.; Matsubara, S.; Kono, H.; Murakami, K.; Itami, K. Synthesis of octagon-containing molecular nanocarbons. *Chem. Sci.* **2022**, *13*, 1848–1868. [CrossRef] [PubMed]
46. Chen, J.-D.; Lu, H.-Y.; Chen, C.-F. Synthesis and structures of multifunctionalized helicenes and dehydrohelicenes: An efficient route to construct cyan fluorescent molecules. *Chem. Eur. J.* **2010**, *16*, 11843–11846. [CrossRef] [PubMed]
47. Zhai, L.; Shukla, R.; Rathore, R. Oxidative C−C bond formation (Scholl reaction) with DDQ as an efficient and easily recyclable oxidant. *Org. Lett.* **2009**, *11*, 3474–3477. [CrossRef] [PubMed]
48. Pieters, G.; Gaucher, A.; Prim, D.; Besson, T.; Planas, J.G.; Teixidor, F.; Viñas, C.; Light, M.E.; Hursthouse, M.B. Binaphthyl platform as starting materials for the preparation of electron rich benzo [g, h, i] perylenes. Application to molecular architectures based on amino benzo [g, h, i] perylenes and carborane combinations. *Chem. Commun.* **2011**, *47*, 7725–7727. [CrossRef] [PubMed]
49. Shen, C.; Zhang, G.; Ding, Y.; Yang, N.; Gan, F.; Crassous, J.; Qiu, H. Oxidative cyclo-rearrangement of helicenes into chiral nanographenes. *Nat. Commun.* **2021**, *12*, 2786. [CrossRef] [PubMed]
50. Chillier, X.; Boulet, P.; Chermette, H.; Salama, F.; Weber, J. Absorption and emission spectroscopy of matrix-isolated benzo [g, h, i] perylene: An experimental and theoretical study for astrochemical applications. *J. Chem. Phys.* **2001**, *115*, 1769–1776. [CrossRef]

51. Izquierdo-García, P.; Fernández-García, J.M.; Perles, J.; Fernández, I.; Martín, N. Electronic Control of the Scholl Reaction: Selective Synthesis of Spiro vs Helical Nanographenes. *Angew. Chem. Int. Ed.* **2023**, *62*, e202215655. [CrossRef]
52. Stanojkovic, J.; William, R.; Zhang, Z.; Fernández, I.; Zhou, J.; Webster, R.D.; Stuparu, M.C. Synthesis of precisely functionalizable curved nanographenes via graphitization-induced regioselective chlorination in a mechanochemical Scholl Reaction. *Nat. Commun.* **2023**, *14*, 803. [CrossRef]
53. Bruckmann, A.; Krebs, A.; Bolm, C. Organocatalytic reactions: Effects of ball milling, microwave and ultrasound irradiation. *Green Chem.* **2008**, *10*, 1131–1141. [CrossRef]
54. James, S.L.; Adams, C.J.; Bolm, C.; Braga, D.; Collier, P.; Friščić, T.; Grepioni, F.; Harris, K.D.M.; Hyett, G.; Jones, W.; et al. Mechanochemistry: Opportunities for new and cleaner synthesis. *Chem. Soc. Rev.* **2012**, *41*, 413–447. [CrossRef] [PubMed]
55. Ralphs, K.; Hardacre, C.; James, S.L. Application of heterogeneous catalysts prepared by mechanochemical synthesis. *Chem. Soc. Rev.* **2013**, *42*, 7701–7718. [CrossRef]
56. Hernández, J.G.; Bolm, C. Altering Product Selectivity by Mechanochemistry. *J. Org. Chem.* **2017**, *82*, 4007–4019. [CrossRef] [PubMed]
57. Andersen, J.; Mack, J. Mechanochemistry and organic synthesis: From mystical to practical. *Green Chem.* **2018**, *20*, 1435–1443. [CrossRef]
58. Andersen, J.M.; Mack, J. Decoupling the Arrhenius equation via mechanochemistry. *Chem. Sci.* **2017**, *8*, 5447–5453. [CrossRef]
59. Ardila-Fierro, K.J.; Hernández, J.G. Sustainability assessment of mechanochemistry by using the twelve principles of green chemistry. *ChemSusChem* **2021**, *14*, 2145–2162. [CrossRef]
60. Rasmussen, M.O.; Axelsson, O.; Tanner, D. A Practical Procedure for the Solid-Phase Synthesis of Racemic 2,2′-Dihydroxy-1,1′-binaphthyl. *Synth. Commun.* **1997**, *27*, 4027–4030. [CrossRef]
61. Zhu, X.; Hua, Y.; Tian, C.; Abney, C.W.; Zhang, P.; Jin, T.; Liu, G.; Browning, K.L.; Sacci, R.L.; Veith, G.M.; et al. Accelerating Membrane-based CO_2 Separation by Soluble Nanoporous Polymer Networks Produced by Mechanochemical Oxidative Coupling. *Angew. Chem. Int. Ed.* **2018**, *57*, 2816–2821. [CrossRef]
62. Howard, J.L.; Brand, M.C.; Browne, D.L. Switching chemoselectivity: Using mechanochemistry to alter reaction kinetics. *Angew. Chem. Int. Ed.* **2018**, *57*, 16104–16108. [CrossRef]
63. Báti, G.; Csókás, D.; Yong, T.; Tam, S.M.; Shi, R.R.S.; Webster, R.D.; Pápai, I.; García, F.; Stuparu, M.C. Mechanochemical Synthesis of Corannulene-Based Curved Nanographenes. *Angew. Chem. Int. Ed.* **2020**, *59*, 21620–21626. [CrossRef] [PubMed]
64. Mori, T. Chiroptical properties of symmetric double, triple, and multiple helicenes. *Chem. Rev.* **2021**, *121*, 2373–2412. [CrossRef] [PubMed]
65. Tian, Y.-H.; Park, G.; Kertesz, M. Electronic structure of helicenes, C_2S helicenes, and thiaheterohelicenes. *Chem. Mater.* **2008**, *20*, 3266–3277. [CrossRef]
66. Hong, J.; Xiao, X.; Liu, H.; Dmitrieva, E.; Popov, A.A.; Yu, Z.; Li, M.-D.; Ohto, T.; Liu, J.; Narita, A.; et al. Controlling the emissive, chiroptical, and electrochemical properties of double [7] helicenes through embedded aromatic rings. *Chem. Eur. J.* **2022**, *28*, e202202243. [CrossRef] [PubMed]
67. Salem, M.S.H.; Sabri, A.; Khalid, M.I.; Sasai, H.; Takizawa, S. Two-Step Synthesis, Structure, and Optical Features of a Double Hetero[7]helicene. *Molecules* **2022**, *27*, 9068. [CrossRef] [PubMed]
68. Yang, W.-W.; Shen, J.-J. Multiple Heterohelicenes: Synthesis, Properties and Applications. *Chem. Eur. J.* **2022**, *28*, e202202069. [CrossRef]
69. Oda, S.; Kawakami, B.; Yamasaki, Y.; Matsumoto, R.; Yoshioka, M.; Fukushima, D.; Nakatsuka, S.; Hatakeyama, T. One-shot synthesis of expanded heterohelicene exhibiting narrowband thermally activated delayed fluorescence. *J. Am. Chem. Soc.* **2021**, *144*, 106–112. [CrossRef]
70. Matsuo, Y.; Maeda, C.; Tsutsui, Y.; Tanaka, T.; Seki, S. Synthesis of closed-Heterohelicenes Interconvertible between Their Monomeric and Dimeric Forms. *Angew. Chem. Int. Ed.* **2023**, *62*, e202314968. [CrossRef]
71. Wynberg, H.; Groen, M.B.; Schadenberg, H. Synthesis and resolution of some heterohelicenes. *J. Org. Chem.* **1971**, *36*, 2797–2809. [CrossRef]
72. Fujikawa, T.; Segawa, Y.; Itami, K. Laterally π-extended dithia[6]helicenes with heptagons: Saddle-helix hybrid molecules. *J. Org. Chem.* **2017**, *82*, 7745–7749. [CrossRef]
73. Chen, F.; Tanaka, T.; Mori, T.; Osuka, A. Synthesis, structures, and optical properties of azahelicene derivatives and unexpected formation of azahepta[8]circulenes. *Chem. Eur. J.* **2018**, *24*, 7489–7497. [CrossRef] [PubMed]
74. Matsuo, Y.; Chen, F.; Kise, K.; Tanaka, T.; Osuka, A. Facile synthesis of fluorescent hetero [8] circulene analogues with tunable solubilities and optical properties. *Chem. Sci.* **2019**, *10*, 11006–11012. [CrossRef] [PubMed]
75. Lousen, B.; Pedersen, S.K.; Bols, P.S.; Hansen, K.H.; Pedersen, M.R.; Hammerich, O.; Bondarchuk, S.; Minaev, B.; Baryshnikov, G.V.; Ågren, H.; et al. Compressing a non-planar aromatic heterocyclic [7]helicene to a planar hetero[8]circulene. *Chem. Eur. J.* **2020**, *26*, 4935–4940. [CrossRef]
76. Maeda, C.; Nomoto, S.; Akiyama, K.; Tanaka, T.; Ema, T. Facile synthesis of azahelicenes and diaza[8]circulenes through the intramolecular Scholl reaction. *Chem. Eur. J.* **2021**, *27*, 15699–15705. [CrossRef] [PubMed]
77. Kumar, A.; Sasai, H.; Takizawa, S. Atroposelective Synthesis of C–C Axially Chiral Compounds via Mono-and Dinuclear Vanadium Catalysis. *Acc. Chem. Res.* **2022**, *55*, 2949–2965. [CrossRef] [PubMed]

78. Sako, M.; Higashida, K.; Kamble, G.T.; Kaut, K.; Kumar, A.; Hirose, Y.; Zhou, D.-Y.; Suzuki, T.; Rueping, M.; Maegawa, T.; et al. Chemo-and enantioselective hetero-coupling of hydroxycarbazoles catalyzed by a chiral vanadium(v) complex. *Org. Chem. Front.* **2021**, *8*, 4878–4885. [CrossRef]
79. Kamble, G.T.; Salem, M.S.H.; Abe, T.; Park, H.; Sako, M.; Takizawa, S.; Sasai, H. Chiral Vanadium(V)-catalyzed Oxidative Coupling of 4-Hydroxycarbazoles. *Chem. Lett.* **2021**, *50*, 1755–1757. [CrossRef]
80. Salem, M.S.H.; Kumar, A.; Sako, M.; Abe, T.; Takizawa, S.; Sasai, H. Preparation of optically pure dinuclear cobalt(III) complex with Λ-configuration as a dianionic chiral catalyst. *Heterocycles* **2021**, *103*, 225–230.
81. Salem, M.S.H.; Takizawa, S. New anionic cobalt(III) complexes enable enantioselective synthesis of spiro-fused oxazoline and iodoacetal derivatives. *Front. Chem.* **2022**, *10*, 34291. [CrossRef]
82. Salem, M.S.H.; Dubois, C.; Takamura, Y.; Kitajima, A.; Kawai, T.; Takizawa, S.; Kirihara, M. Light-induced autoxidation of aldehydes to peracids and carboxylic acids. *Green Chem.* **2024**, *26*, 375–383. [CrossRef]
83. Salem, M.S.H.; Khalid, M.I.; Sako, M.; Higashida, K.; Lacroix, C.; Kondo, M.; Takishima, R.; Taniguchi, T.; Miura, M.; Vo-Thanh, G.; et al. Electrochemical synthesis of hetero[7]helicenes containing pyrrole and furan rings via an oxidative heterocoupling and dehydrative cyclization sequence. *Adv. Synth. Catal.* **2023**, *365*, 373–380. [CrossRef]
84. Salem, M.S.H.; Sharma, R.; Khalid, M.I.; Sasi, M.; Amasaki, R.; Imai, Y.; Arisawa, M.; Takizawa, S. Data-driven Electrochemical One-pot Synthesis of Double Hetero[7]dehydrohelicene. *Electrochemistry* **2023**, *91*, 112015. [CrossRef]
85. Kondo, M.; Wathsala, H.D.P.; Salem, M.S.H.; Ishikawa, K.; Hara, S.; Takaai, T.; Washio, T.; Sasai, H.; Takizawa, S. Bayesian optimization-driven parallel-screening of multiple parameters for the flow synthesis of biaryl compounds. *Commun. Chem.* **2022**, *5*, 148. [CrossRef] [PubMed]
86. Kondo, M.; Sugizaki, A.; Khalid, M.I.; Wathsala, H.D.P.; Ishikawa, K.; Hara, S.; Takaai, T.; Washio, T.; Takizawa, S.; Sasai, H. Energy-, time-, and labor-saving synthesis of α-ketiminophosphonates: Machine-learning-assisted simultaneous multiparameter screening for electrochemical oxidation. *Green Chem.* **2021**, *23*, 5825–5831. [CrossRef]
87. Liu, C.; Zhang, S.; Li, J.; Wei, J.; Müllen, K.; Yin, M. A Water-Soluble, NIR-Absorbing Quaterrylenediimide Chromophore for Photoacoustic Imaging and Efficient Photothermal Cancer Therapy. *Angew. Chem. Int. Ed.* **2019**, *58*, 1638–1642. [CrossRef]
88. Lin, H.-A.; Sato, Y.; Segawa, Y.; Nishihara, T.; Sugimoto, N.; Scott, L.T.; Higashiyama, T.; Itami, K. A Water-Soluble Warped Nanographene: Synthesis and Applications for Photoinduced Cell Death. *Angew. Chem. Int. Ed.* **2018**, *57*, 2874–2878. [CrossRef]

Disclaimer/Publisher's Note: The statements, opinions and data contained in all publications are solely those of the individual author(s) and contributor(s) and not of MDPI and/or the editor(s). MDPI and/or the editor(s) disclaim responsibility for any injury to people or property resulting from any ideas, methods, instructions or products referred to in the content.